JOURNAL OF PROPULSION AND POWER
Vol. 12, No. 4, July–August 1996

Hot-Spot Ignition of Condensed Phase Energetic Materials

David L. Bonnett* and P. Barry Butler†
University of Iowa, Iowa City, Iowa 52242

A micromechanics approach to hot-spot formation and growth to detonation in condensed-phase energetic materials is presented. A numerical model based on fundamental conservation principles is developed to examine the dynamic and thermodynamic processes that occur in a generalized heterogeneous, energetic material subjected to weak shock loading. The work focuses on the thermal/mechanical processes that act to transfer compression work of the shock wave into localized high-temperature ignition sites. A special interest of this research is to determine the dominant physical processes occurring at different times during hot-spot formation. Processes such as viscoplastic heating, phase change, finite rate condensed-phase decomposition, gas-phase heating, and heat transfer between the void and the condensed-phase are included in the model. Results for cyclotrimethylene trinitramine ($C_3H_6N_6O_6$), a common ingredient in high-energy solid rocket propellants, show that viscoplastic heating is an effective mechanism for producing high-temperature regions in the energetic material adjacent to a shock-collapsed void. Furthermore, it is shown that under certain initial conditions (pore size, shock pressure, etc.), localized heating can lead to the release of chemical energy that exceeds the energy dissipated by heat losses, and that melting and the variation of condensed-phase viscosity and yield strength can greatly affect the dynamics of pore collapse.

Nomenclature

A = reaction rate prefactor, s^{-1}
a = sphere internal radius, m
b = sphere outer radius, m
c_c = specific heat of condensed phase, J/kg-K
c_v = specific heat at constant volume, J/kg-K
E = activation energy, J/mole
HR = heat of reaction, J/kg
I = total number of chemical species, dimensionless
J = total number of chemical reactions, dimensionless
k = thermal conductivity, W/m-K
k_r = reaction rate constant, s^{-1}
N = reaction progress variable, dimensionless
p = pressure, N/m^2
q_{ch} = heat release, W/m^3
R_g = gas constant, J/kg-K
R_u = universal gas constant, J/kmol-K
RR = reaction rate, s^{-1}
r = radius, m
T = temperature, K
t = time, s
u = velocity, m/s
Y = mass fraction, dimensionless
$\bar{Y}$ = plastic yield strength, N/m^2
α_μ = coefficient in Eq. (22), m^2/N
β_m = isobaric expansion coefficient, K^{-1}
δ = thermal boundary-layer thickness, m
η = covolume, m^3/kg
μ = viscosity, kg/m-s
ν = stoichiometric coefficient, dimensionless
ρ = density, kg/m^3
Φ = energy dissipation, W/m^2
ϕ = porosity, dimensionless

Subscripts
b = sphere outer radius
c = condensed phase
g = gas phase
i = interface or chemical species i
k = reaction k
m = melting point
s = shock wave
v = viscous stress
y = yield stress
0 = initial or reference state

Introduction

CONDENSED-PHASE, energetic materials (propellants and explosives) often exhibit a tradeoff between performance, associated with energy content of the material, and the potential for inadvertent ignition and transition to detonation.[1–3] It is well documented that accidental initiation is possible during all phases of the energetic material life cycle, including processing, transportation, testing, handling, and storage.[4] The interest in developing energetic materials that are both high-performance and insensitive to inadvertent ignition has led to a significant quantity of research focused primarily on characterizing the sensitivity of energetic materials to various stimuli (thermal, mechanical, and electrical), and on identifying the mechanisms involved in initiation and detonation. A recent review article by Mellor et al.[3] presented flowcharts illustrating proposed pathways, based on experimental evidence, for various initiation stimuli including: shock, impact, friction, and electrostatic discharge. The present work focuses on ignition from shock compression. Development of methods to predict the hazards associated with current energetic materials, and the incorporation of these methods into the design process for new formulations, is the ultimate goal of much of the previous research.[5] Unfortunately, understanding energetic material initiation mechanisms at a fundamental level is a difficult task. Many of the current test methods are considered inadequate for hazards characterization since they provide little insight into the actual physical processes occurring during initiation.[2] Until the recent development of advanced experimental techniques, most of the previous studies were limited to examining the effects of material parameters, such as porosity, on initiation sensitivity, and on characterizing the ini-

Received July 21, 1995; revision received Feb. 1, 1996; accepted for publication Feb. 19, 1996.

*Graduate Research Assistant, Department of Mechanical Engineering.
†Professor, Department of Mechanical Engineering.

tiation properties of specific energetic materials subjected to different stimuli.[6] Because of the predictive shortcomings in both modeling and experiments, it is highly desirable to develop a model, based on first principles, that can provide an understanding of the fundamental physical processes that occur during the initiation of energetic materials. The research discussed here is based on a micromechanics approach to hot-spot formation and growth to detonation in energetic materials.[7]

A general consensus has emerged from much of the research conducted in the area of shock initiation of heterogeneous energetic materials. The following facts are generally accepted:

1) Initiation in these materials occurs at isolated, high-temperature regions called hot spots.

2) These hot spots are thermal in origin and are usually formed from the interaction of the shock wave with defects in the material.

3) Hot-spot formation depends on the material's mechanical, thermal, and chemical properties.

Hot-spot ignition is observed in high-energy propellant formulations and explosives that have detonated at shock pressures well below the level necessary for thermal ignition from bulk heating alone.[5-8] In some cases, the energy transmitted from a relatively weak shock wave is sufficient to initiate a sustained reaction which, following an induction period, can transition to a high-order detonation. This phenomenon was very clearly demonstrated in the work of Baillou,[9] where several batches of nearly identical nitramine crystals showed significantly different shock ignition thresholds. It was noted in Ref. 9 that the only difference between the samples was the size and quantity of internal voids because of their respective manufacturing processes.

Several thermomechanical mechanisms that have been suggested[10-14] as potential hot-spot sources include: friction between adjacent grains, jetting of material fragments across voids, hydrodynamic pore collapse, viscous heating and internal shear, and shock interactions at density discontinuities. Much of the experimental data and analytical modeling of hot spots indicates that the specific mechanisms responsible for hot-spot formation depend on the physical and thermodynamic properties of the heterogeneous materials, as well as the means by which the energy is transmitted to the material from an external source (e.g., shock, shear, thermal heating, fragment impact, etc.). For low porosity (<10%) shock-impacted nitramines, Khasainov et al.[10] postulate that heating because of plastic work at pore interfaces is the dominant mechanism for hot-spot ignition. Others have contributed to the understanding of viscoplastic heating effects in energetic materials.[15-19] Contention arises, however, in the many different mechanisms of hot-spot generation that have been proposed over the years.[20,21]

It is well known that the introduction of voids in energetic materials causes increased sensitivity to shock ignition. In fact, manufacturers commonly add artificial cavities to increase the detonability of explosives.[22] For this reason, many of the proposed hot-spot models focus on shock-induced void or cavity collapse as the mechanism of hot-spot formation. Hot-spot theories include models of adiabatic compression of gas in a collapsing cavity,[22-29] hydrodynamic cavity collapse,[30,31] viscoplastic heating of the condensed-phase material surrounding a collapsing cavity, development of shear bands in the solid,[25,32-38] and others.[39-41] One model that has had success in predicting some of the previously mentioned features is the viscoplastic pore collapse model. This model originated in the study of bubble collapse in liquids.[42] Carroll and Holt[43] developed a simplified hollow sphere model, similar to the bubble collapse model, to approximate the dynamic compaction behavior of shock-loaded porous metals. Carroll et al.[44] included melting effects and temperature-dependent material yield strength and viscosity. These researchers found that the inclusion of both melting and temperature-dependent properties could result, under certain conditions, in the transition of the pore collapse from a viscous to an inertia dominated collapse, even for pore Reynolds number values less than one. Khasainov and others[45] extended the viscoplastic pore collapse model to include a single Arrhenius-type chemical reaction at the pore surface, mass transfer from the material to the pore gas, and a Arrhenius-type single gas-phase decomposition reaction.

Research suggests that hot-spot formation depends strongly on the microstructural, mechanical, thermal, and chemical properties of the material. Important physical processes involved in hot-spot formation are known to include: heating effects caused by the interaction of the shock wave with a void in an energetic material, melting of the energetic material, heat conduction in the material, and chemical reaction in the material. It is important, therefore, for any predictive model to include these effects. The work reported here focuses on the thermal/mechanical processes that act to transfer compression work of the shock wave into localized high-temperature ignition sites. It is shown that under certain initial conditions (pore size, shock pressure, etc.), localized heating can lead to the release of chemical energy that exceeds the energy dissipated by heat losses. Of special interest in this research is the determination of the dominant physical processes occurring at different times during hot-spot formation. This work is an extension of an earlier effort by Kang et al.[7] with the following improvements: 1) an improved treatment of the hot-spot interface temperature and condensed-phase temperature distribution, 2) introduction of a simplified chemistry model for cyclotrimethylene trinitramine ($C_3H_6N_6O_6$) (RDX) decomposition, and 3) improved treatment of solid–liquid phase change. In addition, a detailed sensitivity study is presented to determine the importance of some poorly characterized physical constants. Hot-spot thermal histories predicted by this model are the direct result of solving basic conservation laws (mass, momentum, and energy) for a small control volume of material adjacent to an internal void that has been shock compressed. While microscopic hot-spot models such as this predict the history of a single hot spot, it should be emphasized they do not relate directly to experimentally measured quantities such as detonation run-up distance or critical diameter. That is, the formation and evolution of a single hot spot cannot uniquely determine the response of the bulk material during shock impact. However, the two are closely coupled through the fundamental hydrodynamic and thermodynamic attributes of the material.

Model Formulation

Before proceeding with the development of a computational model to simulate viscoplastic pore collapse, it is appropriate to list key assumptions made in the present model:

1) An ideal hollow-sphere geometry[43] is used to represent a pore and the energetic material surrounding it. This geometry is shown in Fig. 1, overlaid on a photomicrograph of the RDX crystals previously studied.[8,9]

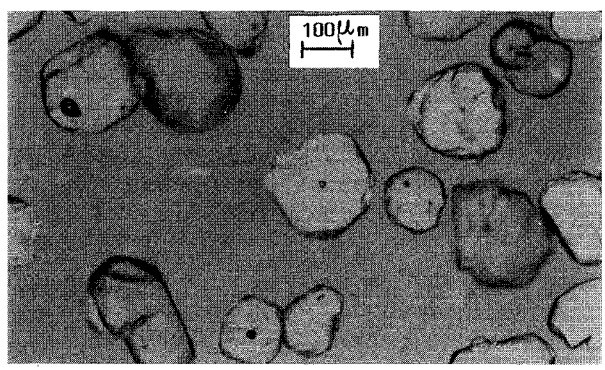

Fig. 1 Illustration of internal voids in commercially manufactured RDX crystals obtained by optical microscopy.[9] In present model pore radius is *a*, and single crystal radius is *b*.

2) The condensed-phase is incompressible and isotropic. Incompressibility is valid for solids subjected to weak shock waves, since very strong shock waves are needed to produce compressibility effects in solids.[46]

3) Flow of the material is spherically symmetric in the vicinity of the void. This is valid when the time required for the shock wave to transit the cavity is small compared to the collapse time.

4) The pressure and temperature are uniform throughout the gas phase, and no chemical reactions occur in the pore gas.

5) The condensed-phase is an ideal, viscoplastic material. This assumption is consistent with the observation of Carroll and Holt[43] that volume changes in the elastic and elastic-plastic phases of collapse are negligible.

6) Thermal conductivities of the gas and condensed-phases are independent of temperature and pressure. In addition, the specific heat of the condensed-phase is also assumed to be temperature and pressure independent.

7) Gas-phase pressure dependence is predicted by a real-gas equation of state. For the high-density gas states possible during the pore collapse, the behavior of the gas phase is likely to deviate substantially from ideal gas behavior.

The resulting mathematical model developed for the control volume shown in Fig. 1 consists of a set of differential equations governing the transient processes occurring in the condensed and gas phases. The behavior of each of these regions is described by the continuity, momentum, and energy equations. These governing equations along with the initial and boundary conditions for the model are described in detail in Ref. 47. The general partial differential equation (PDE) form of the governing equations is subsequently reduced to a set of ordinary differential equations (ODEs) under the assumptions previously listed. Presented here are the final form of the equations solved in the present model:

Motion of the pore interface:

$$\rho_c\{a\,\ddot{a}(1-\phi^{1/3}) + \tfrac{1}{2}\dot{a}[4\dot{a}(1-\phi^{1/3}) - \dot{a}(1-\phi^{4/3})]\} = p_g - p_s - p_v + p_y \tag{1}$$

where

$$p_v = 12a^2\dot{a}\int_a^b \frac{\mu_c}{r^4}\,dr \tag{2}$$

$$p_y = -2\int_a^b \left(\frac{\bar{Y}_c}{r}\right) dr \tag{3}$$

Gas density:

$$\frac{d\rho_g}{dt} = -\frac{3\rho_g\dot{a}}{a} \tag{4}$$

Gas temperature:

$$\frac{dT_g}{dt} = \frac{3}{a\rho_g c_{vg}}\left(k_g\frac{T_{c,i}-T_g}{\delta_g} - p_g\dot{a}\right) \tag{5}$$

Gas-phase equation of state:

$$p_g = \frac{\rho_g R_g T_g}{1-\eta\rho_g} \tag{6}$$

Here, the pore radius a is representative of the average pore size in a much larger sample of material containing multiple, randomly distributed voids. The porosity of the control volume is representative of the macroscopic material porosity, and is defined as

$$\phi = (a/b)^3 \tag{7}$$

where a and b are the inner and outer pore radius, respectively (see Fig. 1).

Integration of the condensed-phase continuity and momentum equations, with the application of the proper interface and boundary conditions leads to an expression for the radial acceleration of the pore interface [Eq. (1)]. Equation (1) is essentially an extension of the classic Rayleigh bubble equation to include the following effects on pore radial motion: variable material viscosity, yield stress, and finite porosity. Including the porosity term in Eq. (1) is necessary to be consistent with the assumption of localized heating in a finite spherical volume surrounding the void.

Likewise, integration of the condensed-phase continuity equation with the substitution of the radial velocity interface condition, gives an expression for the velocity field in the condensed-phase. The resulting expression depends only on the radial position in the condensed phase and the position and velocity of the pore interface:

$$u_c = \dot{a}a^2/r^2 \tag{8}$$

Because the condensed phase is deforming during pore collapse, it is convenient to use a Lagrangian form of the energy equation

$$\rho_c c_c\frac{dT_c}{dt} = k_c\left(\frac{\partial^2 T_c}{\partial r^2} + \frac{2}{r}\frac{\partial T_c}{\partial r}\right) + \Phi_c + q_{ch} \tag{9}$$

with appropriate boundary conditions at $r = b$ (adiabatic) and at the solid-gas interface $r = a$:

$$k_c\frac{\partial T_c}{\partial r}\bigg|_{r=a} = -k_b\frac{(T_g - T_{c,i})}{\delta_g} \tag{10}$$

In Eq. (10), the term dT_c/dt represents the total time derivative of temperature for a point in the condensed-phase material that is convected with its radial motion during pore collapse. The contribution to the rate of temperature change for a Lagrangian particle involves heat release by chemical-reaction q_{ch}, thermal conduction, and viscoplastic dissipation written as

$$\Phi_c = 12\mu_c(u_c^2/r^2) + 2\bar{Y}_c(|u_c|/r) \tag{11}$$

and the energy generated by chemical reactions.

In previous viscoplastic hot-spot modeling,[7,15] an integral transformation method was used to compute interface temperature. This simplified the problem by converting the energy equation into a single integral differential equation and eliminated the need to solve the thermal field in the entire condensed-phase region ($a < r < b$). The integral approach requires the assumption of a thermal profile in the domain. Both exponential and polynomial expressions have been used for this purpose, but their applicability to this problem is questionable. The present work uses a finite difference method to solve the condensed-phase energy equation throughout the domain $a < r < b$. To derive finite difference approximations for the heat conduction derivative appearing in the energy equation, the condensed-phase region was discretized in a coordinate system that translates with the material as it is deformed. Since the condensed phase is assumed to be incompressible, a Lagrangian grid system was ideally suited. Thus, as time evolves, the location of each computational node is determined from the location of the pore interface and mass conservation (i.e., the condensed phase is incompressible, but deforms as the pore collapses).

Constitutive Relations

The general reaction scheme for J reaction steps involving I species can be written as

$$\sum_{i=1}^{I} \nu'_{ij} M_i \rightarrow \sum_{i=1}^{I} \nu''_{ij} M_i \tag{12}$$

for $j = 1$ through J, where ν'_{ij}, ν''_{ij}, and M_i are the stoichiometric coefficients of the reactants and products, and the chemical symbol of the ith species, respectively. The reaction rate for each step is

$$RR_j = k_{r,j} \prod_{i=1}^{I} N_i^{\nu'_{ij}} \tag{13}$$

where N_i is a dimensionless progress variable used to track the creation or destruction of the global species i, and $k_{r,j}$ is the reaction rate coefficient, assumed to obey an Arrhenius type behavior,

$$k_{r,j} = A_j \exp(-E_j/R_u T) \tag{14}$$

Here, A_j and E_j are the jth reaction step pre-exponential factor and activation energy, respectively. Moving with the material in the Lagrangian coordinate system, the rate of change of the progress variable is

$$\frac{dN_i}{dt} = \sum_{j=1}^{J} \nu_{ij} RR_j \tag{15}$$

for species $i = 1, \ldots, I$, where $\nu_{ij} = \nu''_{ij} - \nu'_{ij}$ are the coefficients of each of the j reactions. Finally, the total chemical energy liberated during the reaction q_{ch} is computed from

$$q_{ch} = \sum_{j=1}^{J} HR_j \rho_c RR_j \tag{16}$$

where HR_j is the heat of reaction for reaction step j.

Combustion of nitramines has been studied a great deal in the past 30 years, and several models to predict the decomposition behavior of these materials have been proposed.[48-53] The reaction mechanism used in this research is a global kinetics model developed by Tarver and McGuire.[53] Tarver and McGuire proposed a three-step ($J = 3$) global reaction mechanism with four species ($I = 4$), to model the thermal explosion behavior of confined RDX:

$$A \rightarrow B \tag{17a}$$

$$B \rightarrow 2C \tag{17b}$$

$$2C \rightarrow D \tag{17c}$$

In this three-step model the first reaction step considered is the irreversible, endothermic ($HR_1 = -419$ kJ/kg) decomposition of the global species A (condensed-phase RDX) into an unstable condensed-phase intermediate species B ($3H_2C = N - NO_2$). The second step in this mechanism is the irreversible, exothermic ($HR_2 = 1256$ kJ/kg) decomposition of B, the condensed-phase intermediate, into C, a highly reactive gaseous species ($CH_2O + N_2O$). The third and final global reaction step involves the highly exothermic ($HR_3 = 5023$ kJ/kg) decomposition of the species C, into final gaseous products D (major species include CO, H_2O, and N_2).

Since many energetic materials melt before reaching their ignition temperatures, it is necessary to include the latent heat in the energy equation. The lumped-capacitance method[53-55] is used to model the latent heat effect in the condensed phase. This model is computationally efficient since the need to model a two-phase region with a jump condition and unknown melt location, common to many phase change models, is eliminated. Instead, it is assumed that the melting occurs over a finite temperature range, and an equivalent specific heat that incorporates the latent energy of phase change is allowed to change rapidly over this temperature range.[54] Appearing in Eq. (10), c_c is replaced by an equivalent specific heat that is defined as

$$c_c^* = \frac{\partial h}{\partial T} = c_c + L\delta(T_c - T_m) \tag{18a}$$

where c_c^* is the equivalent specific heat, h is the enthalpy, L is the latent heat of fusion, δ is the Dirac delta function, and T_m is the condensed-phase melt temperature. It is assumed that melting of the condensed phase occurs over a finite temperature range ΔT, and so Eq. (18a) can be replaced by the expression,[54]

$$c_c^* = \frac{\partial h}{\partial T} = c_c + L\delta^*(T_c - T_m, \Delta T) \tag{18b}$$

where the delta function has been approximated by δ^*, which has a finite value when the condensed-phase temperature is within the temperature range $(T_m - \Delta T) > T_c > (T_m + \Delta T)$, and is zero when the temperature is outside of this range. The area under the delta form function is set equal to one by definition of the delta function. The value of ε is arbitrarily set to 2 K in the present model. It is also assumed that the liquid mass fraction varies linearly with temperature over the melting range as

$$Y_L = 0 \quad \text{if} \quad T_c < (T_m - \varepsilon) \tag{19a}$$

$$Y_L = (1/2\varepsilon)[T_c - (T_m - \varepsilon)] \quad \text{if} \quad (T_m - \varepsilon) \le T_c \le (T_m + \varepsilon) \tag{19b}$$

$$Y_L = 1 \quad \text{if} \quad T_c > (T_m + \varepsilon) \tag{19c}$$

To close the hot-spot model several additional relations are needed. These include expressions for the temperature and pressure dependence of the condensed-phase melt temperature, yield strength, and viscosity. Because of the large temperature and pressure variations that may occur during pore collapse, the temperature and pressure dependence of the condensed-phase properties must be considered. The melt temperature is assumed to vary linearly with pressure[19]

$$T_m = T_{m0} + \beta_m P_c \tag{20}$$

where T_{m0} is the melt temperature at atmospheric pressure, β_m is an experimentally determined constant, and P_c is the local condensed-phase stress. A function of r, P_c is found by integrating the condensed-phase momentum equation from the outer control volume radius ($r = b$) to the radial position of interest.

The condensed-phase properties, yield strength and viscosity, play significant roles in both the dynamics of pore collapse and the heating processes that occur during collapse. Note that the yield strength decreases very rapidly in the melting range. The expression for the variation of the condensed-phase yield strength with pressure and temperature is

$$\bar{Y}_c = \bar{Y}_0 \left(\frac{T_m - T_c}{T_m - T_0} \right)^m \quad \text{if} \quad T_c < (T_m - \varepsilon) \tag{21a}$$

$$\bar{Y}_c = (1 - Y_L) \left[\bar{Y}_0 \left(\frac{\varepsilon}{T_m - T_0} \right)^m \right] \quad \text{if} \quad (T_m - \varepsilon) \le T_c \le (T_m + \varepsilon) \tag{21b}$$

$$\bar{Y}_c = 0 \quad \text{if} \quad T_c > (T_m + \varepsilon) \tag{21c}$$

where $\bar{Y}_0$ is the yield strength at atmospheric pressure and an initial temperature of $T_0 = 300$ K. The condensed-phase viscosity in the three temperature regions is

$$\mu_c = \mu_{c0} \exp\left(\alpha_\mu P_c \frac{T_0}{T_c}\right) \quad \text{if} \quad T_c < (T_m - \varepsilon) \tag{22a}$$

$$\mu_c = \mu_{c0} \exp\left[\alpha_\mu P_c \frac{T_0}{(T_m + \varepsilon)} + \frac{E_c}{R_u}\left(\frac{1}{(T_m + \varepsilon)} - \frac{1}{T_m}\right)\right] Y_L + \mu_{c0} \exp\left(\alpha_\mu P_c \frac{T_0}{(T_m - \varepsilon)}\right)(1 - Y_L)$$

$$\text{if} \quad (T_m - \varepsilon) \leq T_c \leq (T_m + \varepsilon) \tag{22b}$$

$$\mu_c = \mu_{c0} \exp\left[\frac{E_c}{R_u}\left(\frac{1}{T_c} - \frac{1}{T_m}\right) + \alpha_\mu P_c \frac{T_0}{T_c}\right]$$

$$\text{if} \quad T_c > (T_m + \varepsilon) \tag{22c}$$

In this equation, μ_{c0} is the condensed-phase viscosity at a pressure of one atmosphere and a temperature of $T_0 = 300$ K, E_c is the condensed-phase activation energy, and α_μ is an experimentally determined constant. Finally, an approximation of the gas phase thermal layer is needed to calculate the heat transfer between the condensed and gas phases. The approximation for the thermal layer thickness $\delta(Fo)$ introduced in Ref. 7 has also been used here.

Results and Discussion

In this section results obtained from the pore collapse model are presented to illustrate some of the important processes involved in hot-spot formation. The global reaction scheme described previously is incorporated into the variable property pore-collapse model to simulate thermal explosion in RDX. For the purposes of this research, thermal explosion is defined as the point at which runaway chemical reactions occur in the condensed phase. Some of the dominant features of hot-spot formation over a range of shock pressures are presented. The effect of pore structural parameters (initial pore radius and initial porosity) on the critical shock pressure required to initiate thermal explosion is discussed, as well as the sensitivity of this critical shock pressure to material properties such as viscosity, yield strength, and condensed and gas-phase thermal conductivities. Unless otherwise stated, all results are taken from simulations that utilize the values shown in Table 1.

Previous work[7] showed that several processes act during pore collapse to influence the temperatures achieved in the condensed phase. At relatively high shock pressures, the early stages of collapse are dominated by viscoplastic heating (which is concentrated near the pore interface), and leads to a rapid increase in the temperature of the condensed-phase RDX adjacent to the pore. The temperature increase in this region (which is large enough to cause melting), results in softening of the material and an increase in pore collapse velocity. The increased collapse velocity leads to rapid pore gas pressurization (and extremely high pore gas temperatures) until the high gas pressure effectively balances the applied shock pressure and the collapse is abruptly terminated. Thermal energy is then transferred from the high temperature pore gas to the lower temperature RDX, raising the condensed-phase temperature near the pore interface above the RDX ignition temperature. In general, as the shock pressure increases, three levels of energetic material response are predicted by the model. These responses are discussed individually.

Decomposition with Quenching of the Reaction

Figures 2 and 3 show the temporal variation of the pore radius, the pore gas pressure, and the pore gas temperature as predicted by the model when the shock pressure is $p_s = 750$ MPa. These results follow the general hot-spot formation sequence described previously, with the pore collapse being terminated abruptly by pore gas pressurization, and high gas temperatures resulting in heat transfer to the lower temperature condensed-phase material at the interface. This heat transfer causes the interface to melt over the period $0.25 < t\ (\mu s) < 0.40$ and then rapidly increase in temperature (see Fig. 4). At the peak temperature (=700 K) RDX decomposition begins. This reaction is shown on the left-hand axis in Fig. 4, as the amount of species A (reaction progress variable N_A) decreases and the concentration of species B (reaction progress variable N_B) increases. However, this endothermic reaction ($A \rightarrow B$), coupled with thermal conduction into the condensed phase, causes the interface temperature to decrease, effectively quenching the reaction. Throughout this process, species C and D are not formed.

Table 1 Initial conditions and constants used in calculations

Variable/constant	Value
A_1	5.76×10^{19} s^{-1}
A_2	4.74×10^{17} s^{-1}
A_3	1.59×10^{15} s^{-1}
a_0	5.0 μm
b_0	13.57 μm
$\dot{a}_0$	0.0 m/s
ϕ_0	0.05, dimensionless
$T_{c0} = T_{g0} = T_0$	300.0 K
P_{g0}	1×10^5 N/m^2
μ_{c0}	50.0 m^2/s
$\bar{Y}_0$	1.1×10^8 N/m^2
ρ_c	1806.0 kg/m^3
c_c	1760.0 J/kg-K
k_c	0.260 W/m-K
k_g	0.083 W/m-K
c_{vg}	714.0 J/kg-K
η	1.0 m^3/kg
T_{m0}	477 K
ε_m	1.0 K
L	1.61×10^5 J/kg
β_m	2.0×10^{-7} K/Pa
m	1, dimensionless
α_μ	1×10^{-10} 1/Pa
E_c	1.93×10^8 J/kmol
E_1/R_u	23,700 K
E_2/R_u	22,200 K
E_3/R_u	17,200 K
HR_1	−419 kJ/kg
HR_2	1,256 kJ/kg
HR_3	5,023 kJ/kg

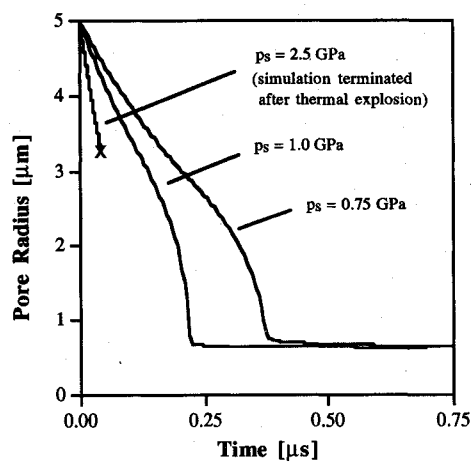

Fig. 2 Temporal variation of pore radius for three shock pressures.

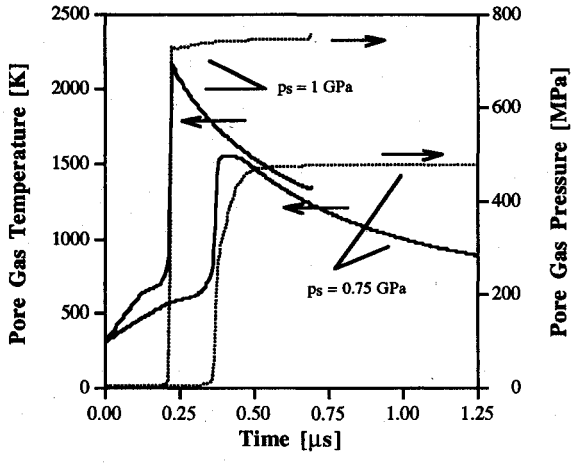

Fig. 3 Temporal variation of pore gas pressure and temperature for shock pressures p_s = 0.75 and 1.0 GPa.

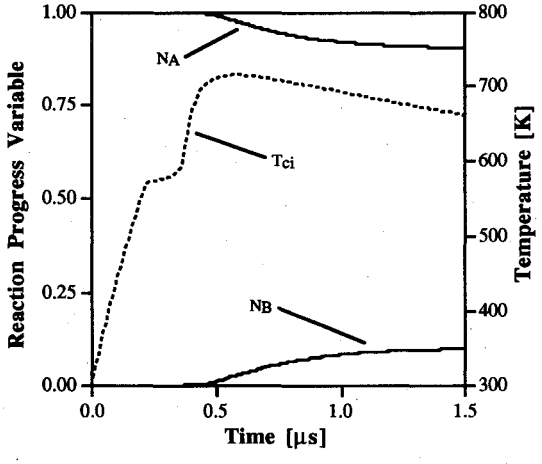

Fig. 4 Temporal variation of pore interface temperature and reaction progress variables for quenched reaction, p_s = 0.75 GPa. Plateau in temperature profile starting at t = 0.2 μs is because of RDX melting.

Thermal Explosion with an Induction Period

The second level of response predicted by the thermal explosion model is illustrated by examining hot-spot formation at a shock pressure of p_s = 1 GPa. Figures 2 and 3 show that the early stages of pore collapse proceed in the same manner as the previous (p_s = 750 MPa) case. However, the increased shock pressure causes a higher pore collapse velocity and a smaller minimum pore volume, resulting in a higher pore gas pressure and temperature after collapse termination. The increased collapse velocity also causes an increase in the magnitude of viscoplastic heating in the condensed phase near the pore interface and results in the RDX melting at $t \approx 0.15$ μs and a higher interface temperature at the time of collapse termination (Fig. 5). Heat transfer from the hot gas to the interface causes a further increase in the interface temperature, which leads to endothermic chemical decomposition of the RDX (reaction step $A \rightarrow B$). This is shown in Fig. 5 as a decrease in the reaction progress variable N_A and an increase in N_B. The chemical energy absorbed by this first reaction step is represented by the curve labeled $q_{ch,1}$ in Fig. 6, which illustrates the heating contribution of each term in the energy equation evaluated at the interface. However, unlike the previous case where radial conduction and the endothermic nature of the first reaction step caused quenching of chemical activity in the condensed phase, Fig. 5 shows that the endothermic reaction $A \rightarrow B$ proceeds to completion, i.e., until $N_A = 0$, and $N_B = 0.8$. At this point the second reaction step, $B \rightarrow C$, begins to release chemical energy (see curve $q_{ch,2}$ in Fig. 6) as species B is converted to species C. For a short period of time, the thermal energy removed by conduction nearly balances the energy produced by this reaction and only a slight increase in the interface temperature occurs. However, the rate of reaction increases as the temperature increases and finally the runaway exothermic reaction $C \rightarrow D$ occurs (curve $q_{ch,3}$ in Fig. 6), causing thermal explosion at the pore interface (Fig. 5).

The relatively long period of time from the collapse termination (and maximum pore gas temperature) to the thermal explosion, the induction time, is controlled by the rate at which chemical energy is generated (or absorbed) by the individual reaction steps and removed by thermal conduction. These processes are, in turn, controlled by the condensed-phase temperature. Immediately following the termination of pore collapse, three mechanisms, 1) the transfer of heat from the hot pore gas to the interface, 2) the conduction of heat from the interface to the condensed phase, and 3) the endothermic reaction $A \rightarrow B$, determine whether the temperature in condensed phase will be high enough to cause runaway chemical reactions. It should be pointed out that the model prediction of the rate of interface temperature rise because of gas phase heat transfer (approximately 200 K in less than 0.1 μs or about 2×10^9 K/s) is extremely high. This physically unrealistic heat transfer rate is a consequence of assuming that the temperature gradient at the pore interface is a linear function of the difference between the interface and mean pore gas temperatures and the gas-phase thermal thickness. During the early stages of pore collapse, when the interface and gas temperatures are nearly equal and little heat transfer occurs between the phases, this assumption is valid. However, a large overprediction of the

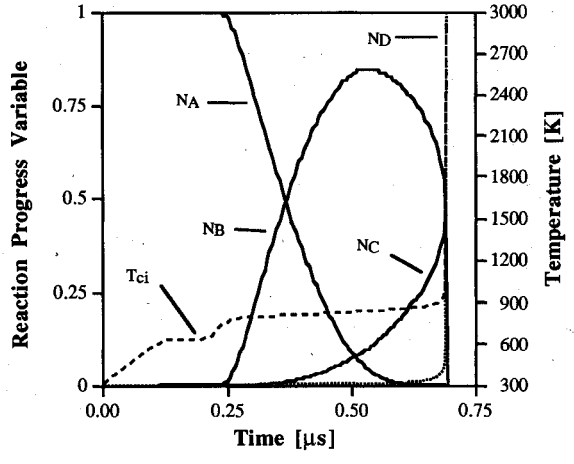

Fig. 5 Temporal variation of pore interface temperature and reaction progress variables for shock pressure, p_s = 1.0 GPa.

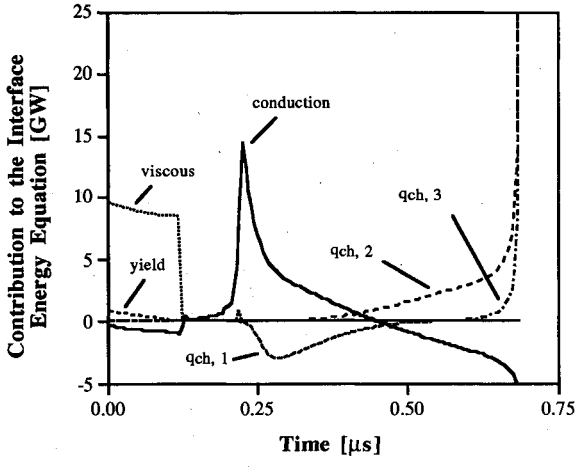

Fig. 6 Temporal variation of the contributions to the interface energy equation. Shock pressure is p_s = 1.0 GPa.

heat transfer rate occurs when gas pressurization produces an extremely high mean pore gas temperature, and therefore, a large difference in interface and pore gas temperatures. Thus, with a better estimate of the interface temperature gradient, the model should predict a slower gas-to-interface heat transfer rate, allowing more time for thermal energy removal radially into the condensed phase via conduction, and possibly resulting in a lower maximum interface temperature. This is significant in predicting ignition thresholds and induction times in energetic materials.

Thermal Explosion with No Induction Period

The third level of response to an increase in shock amplitude is discussed here. In this case (p_s = 2.5 GPa) the pore collapse velocity is much higher than in the previous cases (Fig. 2) and the model simulation is terminated (i.e., thermal explosion occurs) before the pore reaches a minimum value (i.e., before pore gas pressurization can cause abrupt collapse termination). This result can be explained by examining Fig. 7, which shows the temporal variation of the interface heating terms during pore collapse. At this shock pressure, the viscous heating raises the interface temperature to the point (700 K) at which RDX decomposition begins (see Fig. 8). This decomposition temperature is much lower than the pressure-dependent melt temperature (>1000 K) predicted by the model at this shock pressure, and the heat removed by the endothermic reaction (Fig. 7, curve $q_{ch,1}$) is offset by viscous heating as the collapse continues. The energy provided by this heating serves to increase the interface temperature, which initiates heat release by the second reaction (curve $q_{ch,2}$) and leads to thermal explosion at the interface (curve $q_{ch,3}$) and termination of the simulation.

One important physical phenomenon that is expected to affect hot-spot formation in energetic materials, but is ignored in this model, should be mentioned at this point. Experiments have shown that a nearly homogeneous liquid-like layer forms on the surface of RDX during combustion.[48-52] Decomposition and vaporization of condensed-phase RDX in this region cause both reactive RDX vapor and decomposition products to be ejected from this layer into the gas above and gas phase chemical reactions occur. In the thermal explosion model, the species C and D are considered to be gaseous. However, mass transfer between the condensed phase and the pore gas is neglected (i.e., all C and D that are produced are retained in the computational cell). At low shock pressures this mass transfer may not significantly affect the dynamics of the pore collapse since condensed-phase decomposition is predicted to occur after pore collapse termination. However, at higher shock pressures (such as p_s = 2.5 GPa) the model predicts that gasification occurs during pore collapse. In this case, including mass transfer from the condensed phase to the pore gas would cause an increase in the pore gas pressure, which would act to resist pore collapse. Thus, to correctly simulate the dynamics of pore collapse in an energetic material over a large range of shock pressures, mass transfer from chemical decomposition should be included.

A summary of the various levels of energetic material response to increases in shock pressure is presented in Fig. 9. The variation of pore collapse termination time, time to max-

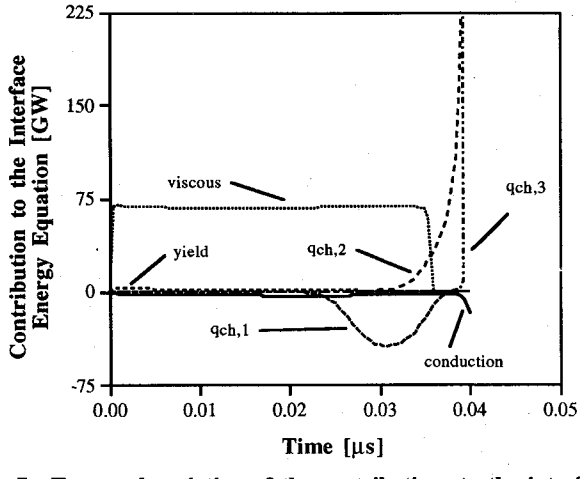

Fig. 7 Temporal variation of the contributions to the interface energy equation. Shock pressure is p_s = 2.5 GPa.

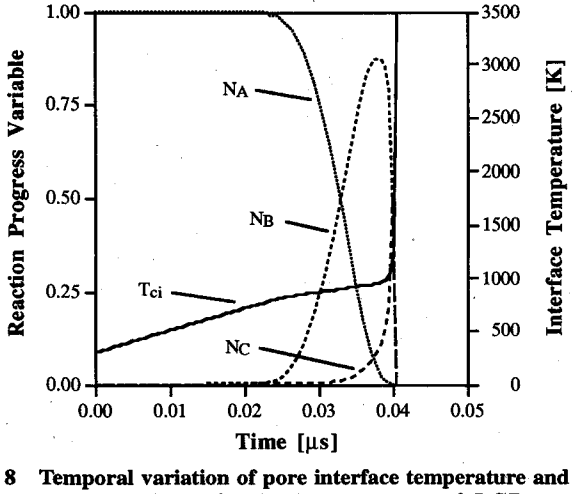

Fig. 8 Temporal variation of pore interface temperature and reaction progress variables for shock pressure, p_s = 2.5 GPa.

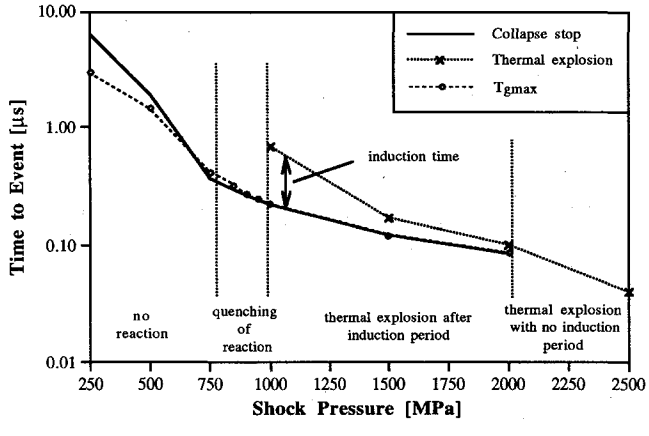

Fig. 9 Variation of pore collapse termination time, time to maximum gas-phase temperature, and thermal explosion time, with shock pressure to illustrate the various levels of response predicted by model.

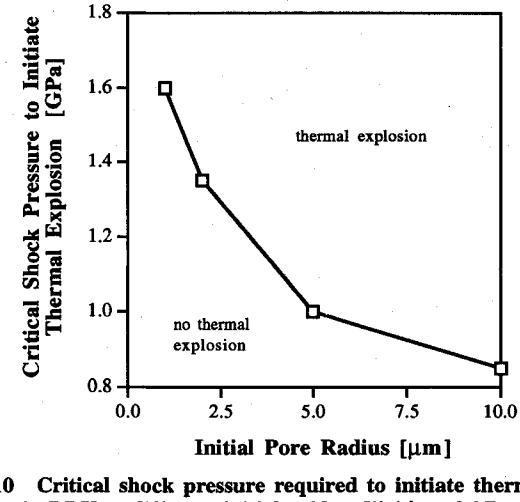

Fig. 10 Critical shock pressure required to initiate thermal explosion in RDX at different initial void radii (ϕ_0 = 0.05).

imum gas-phase temperature, and thermal explosion time, with shock pressure is shown. The minimum shock pressure required to initiate RDX thermal runaway is $p_s = 1000$ MPa. The induction time, defined earlier as the time between pore collapse stop and thermal runaway is seen to decrease with increasing shock pressure until a point is reached when the collapse time and thermal explosion coincide. As mentioned briefly, including mass transfer between the decomposing condensed-phase RDX and the pore gas would likely affect these high shock pressure data. The remainder of this research focuses on determining the critical, that is minimum, shock pressure required to initiate thermal explosion in RDX when some of the important model parameters are varied.

Influence of Structural Parameters

As shown, the response of an energetic material to a shock stimulus is strongly dependent on the magnitude of the applied shock wave. Experimental evidence[8,9,12] has also shown that the physical structure of an energetic material, such as the initial void diameter and initial porosity, greatly influences hot-spot formation in the material. This section examines the effect of these material parameters on the critical shock pressure required to initiate thermal explosion in RDX. Figure 10 illustrates the variation of the critical (thermal explosion) shock pressure with initial void radius for an initial porosity of 5%.

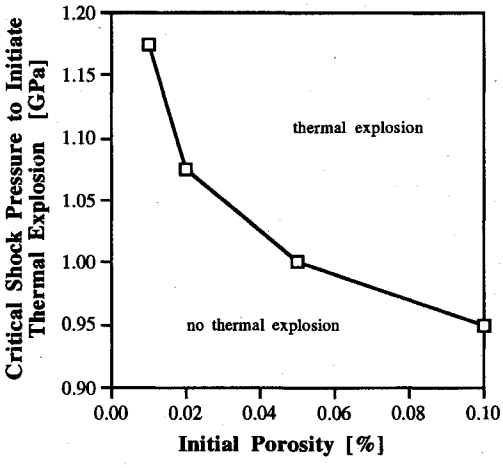

Fig. 11 Critical shock pressure required to initiate thermal explosion in RDX at different initial porosities ($a_0 = 5\mu$m).

At a given initial radius, a shock pressure greater than the critical pressure results in thermal runaway, while shock pressures below the curve cause no explosion. This figure clearly shows that the minimum shock pressure required to initiate thermal explosion in RDX decreases as the initial pore radius increases. This can be explained by examining the magnitude of viscous resistive stress [Eq. (2)] in the momentum equation. It decreases as the pore radius increases. A decrease in the force-resisting pore collapse leads to an increase in the pore collapse velocity, producing high heating rates and high temperatures in the material adjacent to the pore. Chemical decomposition, leading to runaway reactions, may occur at these hot spots.

The relationship between the initial porosity and the critical shock pressure for thermal explosion is demonstrated in Fig. 11 (for an initial pore radius of 5 μm). This shows that the minimum shock pressure required to produce thermal runaway decreases as the initial porosity increases. The inverse relationship between plastic yield resistive stress [Eq. (3)] and porosity is responsible for increased collapse velocities and higher condensed-phase temperatures leading to greater sensitivity to decomposition at the higher porosities.

Thermal Explosion Sensitivity to Material Parameters

Many of the RDX material properties needed to simulate hot-spot formation via the viscoplastic pore collapse model are not well known and consequently many that are used in this research are estimates. In addition, few data exist for these properties at the elevated temperatures and pressures sometimes predicted by the model in these simulations. For these reasons, a study was undertaken to examine the influence many of the important material parameters have on RDX hot-spot formation. Specifically, the thermal explosion threshold pressure sensitivity to changes in the initial values of these properties is examined. The properties chosen for this study correspond to the dominant physical processes that influence thermal runaway in the material. These include the condensed-phase viscosity, yield strength, conductivity, the prefactor for the initial condensed-phase decomposition reaction A_1, and the melting temperature equation coefficient β_m. Also included was the gas-phase thermal conductivity. Results shown in Figs. 12 and 13 illustrate the variation of the critical shock pressure with a corresponding change in the property. All of these results are presented as percentage changes referenced to the base case that uses the initial conditions and property values shown in Table 1.

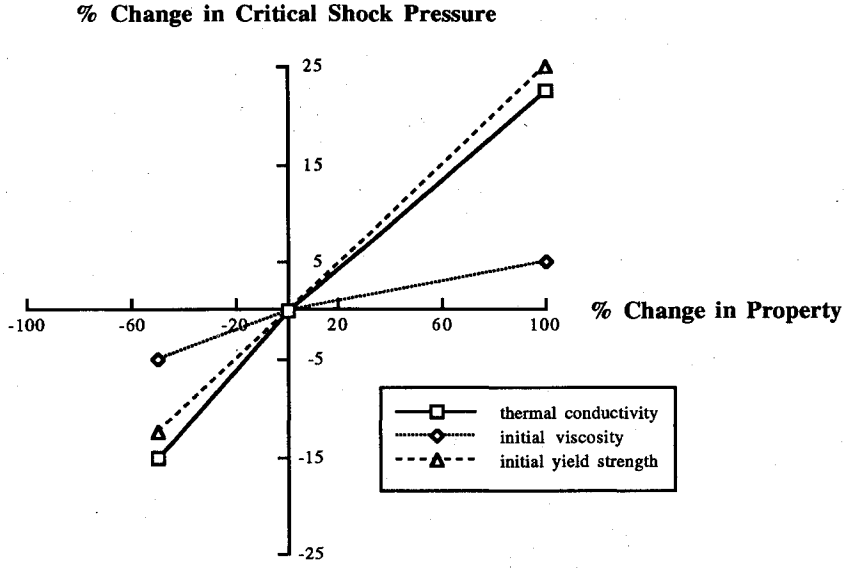

Fig. 12 Sensitivity of the critical shock pressure required to initiate thermal explosion in RDX to changes in condensed-phase viscosity, yield strength, and thermal conductivity.

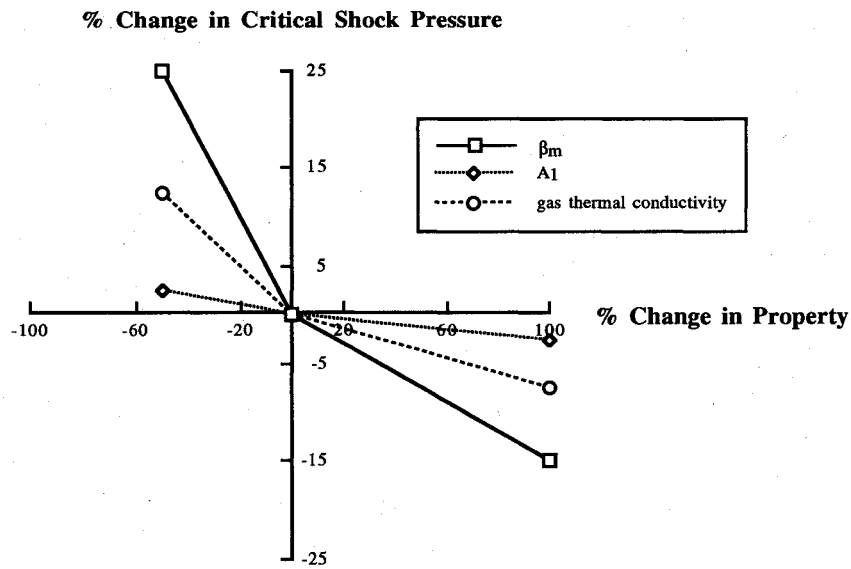

Fig. 13 Sensitivity of the critical shock pressure required to initiate thermal explosion in RDX to changes in β_m, gas phase thermal conductivity, and A_1.

Figure 12 clearly shows that a large increase in the condensed-phase yield strength or viscosity leads to decreased shock sensitivity (shown as an increased critical shock pressure), whereas decreases in these properties cause increased shock sensitivity (decrease in the critical shock pressure). The increase in resistive pressure caused by a higher material yield strength or viscosity acts to slow the rate of pore collapse and therefore to reduce the viscoplastic heating rate near the pore interface. This effect is much more pronounced for large changes in the yield strength. As expected, an increase in the condensed-phase thermal conductivity also greatly affects the critical shock pressure. A large conductivity increase allows heat to be more effectively conducted away from the regions of intense viscoplastic heating near the pore interface where high temperatures may lead to chemical reactions. This leads to a decrease in shock sensitivity.

While increases in the condensed-phase properties mentioned earlier lead to increased critical thermal explosion pressures, increases in the gas-phase thermal conductivity, A_1, and β_m, result in decreased critical thermal explosion pressures as shown in Fig. 13. Very little change in critical shock pressure occurs for large changes in A_1. However, an increase in the gas phase thermal conductivity allows for much more effective heat transfer between a high-temperature pore gas and a lower temperature condensed-phase material at the pore interface. This causes higher interface temperatures to be reached and enhances chemical decomposition, which leads to increased shock sensitivity. Figure 13 shows that the critical shock pressure is most sensitive to β_m. The explanation for this is that β_m determines the variation of the melting temperature with pressure. A large increase in this constant leads to a large increase in the melting temperature, which allows more time for viscoplastic heating to occur (and thus higher temperatures) before the material resistive pressures decrease from melting and the collapse terminates by gas pressurization.

Conclusions and Recommendations

A micromechanical model, based on the fundamental conservation principles, has been developed to examine the dynamic and thermodynamic processes that occur in heterogeneous energetic material subjected to shock impact. The model incorporated condensed-phase viscoplastic heating, melting, property variation with temperature and pressure, and thermal conduction via a finite difference method. A simplified global kinetics model was used to model thermal explosion in the condensed phase. The pore gas temperature and pressure were calculated using an energy balance and a nonideal gas equation of state, respectively. Simulations were performed to examine 1) the importance of several physical processes that occur during void collapse, 2) the role of pore structural parameters on the minimum shock pressure required to initiate thermal explosion in the condensed phase, and 3) the sensitivity of the minimum thermal explosion shock pressure to changes in some of the energetic material properties. From these results several conclusions can be stated:

1) Viscoplastic heating is an effective mechanism for producing high-temperature regions in the energetic material adjacent to a shock-collapsed void. Pore collapse velocity increases with increasing shock pressure and viscous heating dominates the condensed-phase energy equation. Plastic work is the dominant heating source at low shock pressures. Thermal conduction into the condensed phase becomes important when the pore collapse velocity is low.

2) The large temperature increases predicted in the energetic material near the void necessitates the use of temperature and pressure-dependent material properties (viscosity and yield strength) and the incorporation of melting to obtain realistic temperature predictions in the condensed phase.

3) Including melting and variable properties in the model calculations dramatically alters the dynamics of the pore collapse when the condensed-phase temperature approaches the melt temperature. When this occurs, stresses resisting pore collapse greatly decrease, resulting in an increase in collapse velocity and rapid increase in pressure and temperature of the gas, causing an abrupt termination of pore collapse when the high gas pressure balances the shock pressure.

4) Initial porosity and pore diameter strongly influence the minimum pressure required to initiate thermal explosion in the material. The model predicts certain experimentally observed trends, namely an increase in initial pore radius or porosity leads to a lower critical shock threshold.

5) The critical pressure needed to initiate runaway chemical reaction in the energetic material is sensitive to changes in many of the model parameters. Large increases in the condensed-phase thermal conductivity and initial yield strength lead to large increases in the thermal explosion threshold pressure and an increase in the melt temperature exponent causes the minimum shock pressure to decrease.

6) When compared with our previous hot spot model,[7] the present model predicts a lower shock initiation threshold (≈25% lower) for the same initial conditions. A comparison of the results from both models indicates the primary reason

for this difference is in the treatment of mass transfer at the pore interface. The present model does not include mass transport from the RDX into the void, and consequently the rate of pressurization in the pore gas is much lower. A higher pressurization rate slows down pore collapse resulting in a much higher shock pressure to initiate runaway reaction.

As discussed previously, this model has certain limitations that should be addressed in the future if the model is to be incorporated into hydrocodes and used to predict hot-spot growth to detonation. The expression used to model heat transfer between the condensed phase and the pore gas is inadequate when high-temperature differences exist between these phases. At these temperature differences the current model calculates an extremely large interface temperature gradient that predicts physically unrealistic interface heating rates. This expression should be replaced with a better approximation, or the gas phase energy equation should be discretized and solved as is the condensed phase energy equation. Also, gasification of condensed phase during chemical decomposition and mass transfer from condensed-phase to pore gas should be included.

Acknowledgments

This research was sponsored by the United States Army Research Office under Contract DAAL03-91-G-0020. David Mann served as Contract Monitor.

References

[1]Boggs, T. L., "The Thermal Behavior of RDX and HMX," *Fundamentals of Solid-Propellant Combustion*, Vol. 90, Progress in Astronautics and Aeronautics, AIAA, New York, 1984, pp. 121–175.

[2]Mellor, A. M., Mann, D. M., Boggs, T. L., Dickinson, C. W., and Roe, W. E., "Hazard Initiation in Energetic Materials: Status of Technology Assessment," *Combustion Science and Technology*, Vol. 54, Nos. 1–6, 1987, pp. 203–215.

[3]Mellor, A. M., Wiegand, D. A., and Isom, K. B., "Hot Spot Histories in Energetic Materials," *Combustion and Flame*, Vol. 101, No. 1, 1995, pp. 26–35.

[4]Mellor, A. M., Boggs, T. L., Covino, J., Dickinson, C. W., Dreitzler, D., Thorn, L. B., Frey, R. B., Gibson, P. W., Roe, W. E., Kirshenbaum, M., and Mann, D. M., "Research Needs and Plan for Energetic Material Hazard Mitigation," *Combustion Science and Technology*, Vol. 59, Nos. 4–6, 1988, pp. 391–400.

[5]Coffey, C. S., DeVost, V. F., and Woody, D. L., "Towards Developing the Capability to Predict the Hazard Response of Energetic Materials Subjected to Impact," *9th Symposium (International) on Detonation* (Portland, OR), U.S. Office of Naval Research, Arlington, VA, 1989, pp. 965–974.

[6]Setchell, R. E., and Taylor, P. A., "The Effects of Grain Size on Shock Initiation Mechanisms in Hexanitrostilbene (HNS) Explosive," *Dynamics of Shock Waves, Explosions and Detonations*, Vol. 94, Progress in Astronautics and Aeronautics, AIAA, New York, 1984, pp. 350–368.

[7]Kang, J., Butler, P. B., and Baer, M. R., "A Thermomechanical Analysis of Hot Spot Formation in Condensed-Phase, Energetic Materials," *Combustion and Flame*, Vol. 89, No. 2, 1992, pp. 117–139.

[8]Bourne, L., "Influence of Intergranular Cavities of RDX Particle Batches on the Sensitivity of Cast Wax Bonded Explosives," *10th Symposium (International) on Detonation*, Boston, MA, U.S. Office of Naval Research, Arlington, VA, 1993.

[9]Baillou, F., Dartyge, J. M., Spyckerelle, M., and Mala, J., "Influence of Crystal Defects on Sensitivity of Explosives," *10th Symposium (International) on Detonation*, Boston, MA, U.S. Office of Naval Research, Arlington, VA, 1993.

[10]Khasainov, B. A., Borisov, A. A., Ermolaev, B. S., and Korotkov, A. I., "Two-Phase Visco-Plastic Model of Shock Initiation of Detonation in High Density Pressed Explosives," *7th Symposium (International) on Detonation* (Annapolis, MD), U.S. Office of Naval Research, Arlington, VA, 1981, pp. 435–447.

[11]Frey, R. B., "The Initiation of Explosive Charges by Rapid Shear," *7th Symposium (International) on Detonation* (Annapolis, MD), U.S. Office of Naval Research, Arlington, VA, 1981, pp. 36–49.

[12]Taylor, P. A., "The Effects of Material Microstructure on the Shock Sensitivity of Porous Granular Explosives," *8th Symposium (International) on Detonation* (Albuquerque, NM), U.S. Office of Naval Research, Arlington, VA, 1985, pp. 26–34.

[13]Coffey, C. S., "Hot Spot Production by Moving Dislocations in a Rapidly Deforming Crystalline Explosive," *8th Symposium (International) on Detonation* (Albuquerque, NM), U.S. Office of Naval Research, Arlington, VA, 1985, pp. 62–67.

[14]Kim, K., and Sohn, C. H., "Modeling of Reaction Buildup Processes in Shocked Porous Explosives," *8th Symposium (International) on Detonation* (Albuquerque, NM), U.S. Office of Naval Research, Arlington, VA, 1985, pp. 926–933.

[15]Butcher, B. M., Carroll, M. M., and Holt, A. C., "Shock-Wave Compaction of Porous Aluminum," *Journal of Applied Physics*, Vol. 45, No. 9, 1974, pp. 3864–3875.

[16]Khasainov, B. A., Borisov, A. A., and Ermolayev, B. S., "Shock Wave Predetonation Processes in Porous High Explosives," *Shock Waves, Explosions, and Detonations*, Vol. 87, Progress in Astronautics and Aeronautics, New York, 1983, pp. 492–504.

[17]Dunin, S. Z., and Surkov, V. V., "Effects of Energy Dissipation and Melting on Shock Compression of Porous Bodies," *Journal of Applied Mechanics and Technical Physics*, Vol. 23, 1982, pp. 123–134.

[18]Attetkov, A. V., Vlasova, L. N., Selivanov, V. V., and Solov'ev, V. S., "Local Heating of a Material in the Vicinity of a Pore upon its Collapse," *Journal of Applied Mechanics and Technical Physics*, Vol. 25, 1984, pp. 286–291.

[19]Maiden, D. E., "A Model for Calculating the Threshold for Shock Initiation of Pyrotechnics and Explosives," *Proceedings of the 12th International Pyrotechnics Seminar* (Vail, CO), 1986, pp. 813–826.

[20]Field, J. E., "Hot Spot Ignition Mechanisms for Explosives," *Accounts of Chemical Research*, Vol. 25, No. 11, 1992, pp. 489–496.

[21]Field, J. E., Bourne, N. K., Palmer, S. J. P., and Walley, S. M., "Hot-Spot Ignition Mechanisms for Explosives and Propellant," *Philosophical Transactions of the Royal Society of London: Series A*, Vol. 339, 1992, pp. 269–283.

[22]Krishna Mohan, K., Field, J. E., and Swallowe, G. M., "Effects of Physical Inhomogeneities on the Impact Sensitivity of Solid Explosives: A High-Speed Photographic Study," *Combustion Science and Technology*, Vol. 40, 1984, pp. 269–278.

[23]Bowden, F. P., and Yoffee, A. D., *Initiation and Growth of Explosion in Liquids and Solids*, Cambridge Univ. Press, 1952.

[24]Chaudhri, M. M., and Field, J. E., "The Role of Rapidly Compressed Gas Pockets in the Initiation of Condensed Explosives," *Proceedings of the Royal Society of London*, Vol. A340, No. 1620, 1974, pp. 113–128.

[25]Field, J. E., Swallowe, G. M., and Heavens, S. N., "Ignition Mechanisms of Explosives During Mechanical Deformation," *Proceedings of the Royal Society of London*, Vol. A382, No. 1782, 1982, pp. 231–244.

[26]Starkenburg, J., "Ignition of Solid High Explosive by Rapid Compression of an Adjacent Gas Layer," *7th Symposium (International) on Detonation* (Annapolis, MD), U.S. Office of Naval Research, Arlington, VA, 1981, pp. 3–16.

[27]Bourne, N. K., and Field, J. E., "Shock-Induced Collapse of Single Cavities in Liquids," *Journal of Fluid Mechanics*, Vol. 244, 1992, pp. 225–240.

[28]Partom, Y., "A Void Collapse Model for Shock Initiation," *7th Symposium (International) on Detonation* (Annapolis, MD), U.S. Office of Naval Research, Arlington, VA, 1981, pp. 506–516.

[29]Frey, R. B., "Cavity Collapse in Energetic Materials," *8th Symposium (International) on Detonation* (Albuquerque, NM), U.S. Office of Naval Research, Arlington, VA, 1985, pp. 68–80.

[30]Mader, C. L., "Initiation of Detonation by the Interaction of Shocks with Density Discontinuities," *Physics of Fluids*, Vol. 8, No. 10, 1965, pp. 1811–1816.

[31]Mader, C. L., "Numerical Modelling of Detonations," *Los Alamos Series in Basic and Applied Science*, Univ. of California Press, 1979.

[32]Chaudhri, M. M., "The Initiation of Fast Decomposition in Solid Explosives by Fracture, Plastic Flow, Friction, and Collapsing Voids," *Preprints of 9th Symposium (International) on Detonation* (Portland, OR), U.S. Office of Naval Research, Arlington, VA, 1989, pp. 331–339.

[33]Field, J. E., Parry, M. A., Palmer, S. J. P., and Huntley, J. M., "Deformation and Explosive Properties of HMX Powders and Polymer Explosives," *9th Symposium (International) on Detonation* (Portland, OR), U.S. Office of Naval Research, Arlington, VA, 1989, pp. 771–780.

[34]Grady, D. E., and Kipp, M. E., "The Growth of Unstable Thermoplastic Shear with Application to Steady-Wave Shock Compression in Solids," *Journal of Mechanics and Physics of Solids*, Vol. 35, 1987, pp. 95–100.

[35]Krishna Mohan, V., Jyothi Bhasu, V. C., and Field, J. E., "Role of Adiabatic Shear Bands in Initiation of Explosives by Drop Weight Impact," *9th Symposium (International) on Detonation* (Portland, OR),

U.S. Office of Naval Research, Arlington, VA, 1989, pp. 557–564.
[36]Boyle, V., Frey, R., and Blake, O., "Combined Pressure Shear Ignition of Explosives," *Preprints of 9th Symposium (International) on Detonation* (Portland, OR), U.S. Office of Naval Research, Arlington, VA, 1989, pp. 1–11.
[37]Coffey, C. S., "Initiation of Explosive Crystals by Shock or Impact," *Preprints of 9th Symposium (International) on Detonation* (Portland, OR), U.S. Office of Naval Research, Arlington, VA, 1989, pp. 864–870.
[38]Tokmakoff, A., Fayer, M. D., and Dlott, D. D., "Chemical Reaction Initiation and Hot-Spot Formation in Shocked Energetic Materials," *Journal of Physical Chemistry*, Vol. 97, 1993, pp. 1901–1913.
[39]Lee, E. L., and Tarver, C. M., "Phenomenological Model of Shock Initiation in Heterogeneous Explosives," *Physics of Fluids*, Vol. 23, No. 12, 1980, pp. 2362–2372.
[40]Tang, P., "A Study of Detonation Processes in Heterogeneous High Explosives," *Journal of Applied Physics*, Vol. 63, No. 4, 1988, pp. 1041–1045.
[41]Tang, P. K., Johnson, J. N., and Forest, C. A., "Modeling Heterogeneous High Explosive Burn with an Explicit Hot Spot Process," *8th Symposium (International) on Detonation* (Albuquerque, NM), U.S. Office of Naval Research, Arlington, VA, 1985, pp. 52–61.
[42]Rayleigh, L., "On the Pressure Developed in a Liquid During the Collapse of a Spherical Cavity," *Philosophical Magazine*, Vol. 34, No. 200, 1917, pp. 94–98.
[43]Carroll, M. M., and Holt, A. C., "Static and Dynamic Pore-Collapse Relations for Ductile Porous Materials," *Journal of Applied Physics*, Vol. 43, No. 4, 1972, pp. 1626–1635.
[44]Carroll, M. M., Kim, K. T., and Nesterenko, V. F., "The Effect of Temperature on Viscoplastic Pore Collapse," *Journal of Applied Physics*, Vol. 59, No. 6, 1986, pp. 1962–1967.
[45]Khasainov, B. A., Attetkov, A. V., Borisov, A. A., Ermolayev, B. S., and Soloviev, V. S., "Critical Conditions for Hot Spot Evolution in Porous Explosives," *Dynamics of Explosions*, Vol. 114, Progress in Astronautics and Aeronautics, AIAA, Washington, DC, 1988, pp. 303–321.
[46]Graham, R. A., *Solids Under High-Pressure Shock Compression*, Springer–Verlag, New York, 1993.
[47]Bonnett, D., and Butler, P. B., "A Thermochemical Model for Analysis of Hot Spot Formation in Energetic Materials," Univ. of Iowa, UIME PBB95-003, Iowa City, IA, 1995.
[48]Cohen, N. S., Lo, G. A., and Crowley, J. C., "Model and Chemistry of HMX Combustion," *AIAA Journal*, Vol. 23, No. 2, 1985, pp. 276–282.
[49]Mitani, T., and Williams, F. A., "A Model for the Deflagration of Nitramines," Sandia National Labs. Rept. SAND86-8230, Albuquerque, NM, Dec. 1986.
[50]Ben-Reuven, M., and Caveny, L. H., "Nitramine Flame Chemistry and Deflagration Interpreted in Terms of a Flame Model," *AIAA Journal*, Vol. 19, No. 10, 1981, pp. 1276–1285.
[51]Li, S. C., Williams, F. A., and Margolis, S. B., "Effects of Two-Phase Flow in a Model for Nitramine Deflagration," *Combustion and Flame*, Vol. 80, Nos. 3,4, 1990, pp. 329–349.
[52]Margolis, S. B., Williams, F. A., and Armstrong, R. C., "Influence of Two-Phase Flow in the Deflagration of Homogeneous Solids," *23th JANNAF Combustion Meeting*, Chemical Propulsion Information Agency Publication 457, Vol. I, 1986, pp. 203–211.
[53]McGuire, R. R., and Tarver, C. M., "Chemical Decomposition Models for the Thermal Explosion of Confined HMX, TATB, RDX, and TNT Explosives," *7th Symposium (International) on Detonation* (Annapolis, MD), U.S. Office of Naval Research, Arlington, VA, 1981, pp. 56–64.
[54]Hobbs, M. L., "XCHEM User's Manual," Sandia National Labs. Rept. SAND93-1603, Albuquerque, NM, 1993.
[55]Yao, L. S., and Prusa, J., "Melting and Freezing," *Advances in Heat Transfer*, edited by J. P. Harnett and T. F. Irvine, Vol. 19, Academic, New York, 1989.